Appl Biochem Biotechnol (2011) 163:813–825
DOI 10.1007/s12010-010-9085-y

A Novel Magneto-fluorescent Nano-bioprobe for Cancer Cell Targeting, Imaging and Collection

Yicheng Wu · Maoquan Chu · Bizhi Shi · Zonghai Li

Received: 1 June 2010 / Accepted: 7 September 2010 /
Published online: 16 October 2010

Abstract Silica-coated magnetic polystyrene nanospheres (MPN) containing CdTe/CdS quantum dots (QDs) and Fe_3O_4 nanoparticles were prepared, and novel anti-EGFR antibodies were conjugated onto these magneto-fluorescent nanocomposites (MPN–QDs–SiO_2) for cancer cell targeting, imaging and collection. Transmission electron microscopy (TEM), scanning electron microscopy (SEM) images and energy-dispersive x-ray spectrometry (EDS) data showed that the MPN had been successfully coated with QDs and a silica shell, and the nanocomposites obtained with negative charged surfaces were well dispersed. The bioconjugates could be used for specifically labeling and separating cancer cells (MDA-MB-435S, SMMC-7721), but did not recognize and separate the K562 cells because the human epidermal growth factor receptor (EGFR) was not expressed on the surface. Because the anti-EGFR antibody, which we have developed, could specifically recognize certain cancer cells that highly expressed EGFR on their surface, these nanoscale bioconjugates, synchronously exhibiting fluorescence and magnetism, may be used in novel bioprobes for labeling and collecting rare cancer cells, which may be beneficial for early cancer diagnosis.

Y. Wu · M. Chu
School of Life Science and Technology, Tongji University, Shanghai 200092,
People's Republic of China

M. Chu (✉)
Institute for Advanced Materials and Nano Biomedicine, Tongji University, Shanghai 200092,
People's Republic of China
e-mail: mqchu98@tongji.edu.cn

B. Shi · Z. Li
State Key Laboratory of Oncogenes and Related Genes, Shanghai Cancer Institute, Shanghai,
People's Republic of China

Z. Li (✉)
School of Medicine, Shanghai JiaoTong University, Shanghai 200032, People's Republic of China
e-mail: zonghaili@shsci.org

Keywords Quantum dots · Magnetic nanospheres · Silica shell · Antibody · Cancer cell

Introduction

Fluorescent and magnetic materials are very useful in biomedical applications. As such, representative materials such as quantum dots (QDs) and ferric oxide nanoparticles have captivated the interest of many scientists during the past decades owing to their interesting optical and magnetic properties. For QDs, these nanomaterials exhibit broad and continuous absorption, narrow and symmetric fluorescence emission, and bright and stable fluorescence, all of which have great potential applications for in vitro biolabeling and in vivo targeting and imaging [1–3]. For magnetic nanoparticles, these nanomaterials can be used for bioseparation, immobilization of cells and enzymes, drug delivery, magnetic resonance imaging and thermotherapy [4–6]. If a nanocomposite synchronously contains QDs and magnetic nanoparticles, this magneto-fluorescent particle with multiple functions may have great potential application in biomedical research areas.

In recent years, a nanocomposite synchronously containing QDs and magnetic nanoparticles has been reported [7–10]. For example, QDs were immobilized on the surface of superparamagnetic polystyrene nanospheres, and the unique combination of fluorescence emission and hyperthermia engineered into these nanocomposites is anticipated for use in clinical applications for simultaneous *in vivo* imaging and local therapy via hyperthermia [8]. As another example, glutathione modified Fe_3O_4-CdSe heterodimers prepared by growing CdSe QDs on the Fe_3O_4 nanoparticles could be moved in living cells by a magnetic moment, which can be observed by the QD fluorescence, and this strategy may offer a useful tool to investigate the difference between the apical and basolateral domains in polarized cells by the asymmetric localization of magnetic nanoparticles that carry specific ligands [9]. When antibodies or peptides are conjugated onto these magneto-fluorescent nanocomposites, these bioconjugates can be used for targeting imaging, specifically separation [10], but also in other biomedical applications.

In this study, we prepared a novel magneto-fluorescent nanocomposite by modifying the magnetic polystyrene nanospheres (MPN) with QDs using electrostatic adsorption, and then coating the MPN–QDs with a silica shell (designated MPN–QDs–SiO_2). Anti-EGFR antibodies 12H23 developed by us were then conjugated onto this nanocomposite for cell imaging and separation. We know that the overexpression of EGFR and EGFRvIII has been found in many epithelial tumors and is often correlated with a worsening of the clinical prognosis [11–13]. Currently, two anti-EGFR antibodies (cetuximab and panitumumab) have been approved for treating colorectal cancer. However, both of them recognize EGFR expressed in cancer cells as well as normal cells [14, 15]. Unlike the two antibodies, monoclonal antibody 806 is an antibody that selectively recognizes the untethered form of EGFR (overexpressed EGFR and EGFRvIII) [16]. In phase I clinical trials, ^{111}I-ch806 (chimeric antibody 806) was observed to specifically locate in target lesions of all patients at all dose levels [17]. Recently, we developed a monoclonal antibody (12H23) that recognizes the same epitope (^{287}CGADSYEMEEDGVRKC^{302}) of mAb 806 [18]. To specifically detect tumor cells, we used mAb 12H23 as the targeting moiety. Because the antibodies used in this work can specifically recognize tumor cells in certain tumors but cannot recognize normal cells, the novel nano-bioconjugates prepared in this work may be of interest for biologists.

Materials and Methods

Materials

The carboxyl-modified MPN was a gift from Professor Yihua Zhu (East China University of Science and Technology). The anti-EGFR monoclonal antibodies (mAb) 12H23 were developed by our group (unpublished data). The QDs with a CdTe core and a CdS shell were synthesized in an aqueous solution (pH 9.0, 95 °C, N_2 atmosphere protection) using $CdCl_2$, fresh NaHTe (NaHTe was prepared by dissolving Te powder into an $NaBH_4$ solution under an N_2 atmosphere), Na_2S and 3-mercaptopropionic acid (MPA) as precursors. The molar ratio of Cd/Te/S/MPA in the reaction solution was about 1:0.5:0.012:4.16 as previously reported [19]. The silane coupling agent, KH-550, was purchased from the Shanghai Yaohua Chemical Plant. Poly(diallyldimethylammonium chloride) (PDADMAC, 40 wt.% in H_2O, MW $= 7 \times 10^5 - 1 \times 10^6$) was purchased from Shanghai Hengyi Chemical Engineering Corporation. Tetraethyl orthosilicate (TEOS), glutaraldehyde solution (25%), ethanol and other reagents, such as $CdCl_2$ and Te powder, were purchased from the Sinopharm Chemical Reagent Co. Ltd. RPMI-1640 culture medium and fetal calf serum (FCS) were obtained from Gibco (USA). Leibovitz's L-15 medium, human breast cancer cells (MDA-MB-453S), liver cancer cells (SMMC-7721) and leukemia cells (K562) were ordered from the Chinese Academy of Sciences. The water used in all experiments was prepared using an ultrapure water system (Molgeneral220a).

Preparation of MPN–QDs–SiO2 Nanocomposites

A schematic illustration of the formation of nanocomposites is shown in Fig. 1. For a typical experiment, PDADMAC aqueous solution (100 μl, 0.5%) containing sodium chloride (1%) was mixed with an MPN suspension (10 μl, 50 pmol/l) and sonicated for 30 min. The mixture was then precipitated by centrifugation and washed three times with water to remove the free PDADMAC. A QDs aqueous solution (200 μl, approximately 1.2 μmol/l) was then mixed with the precipitates and sonicated for 30 min. The mixture was also precipitated and

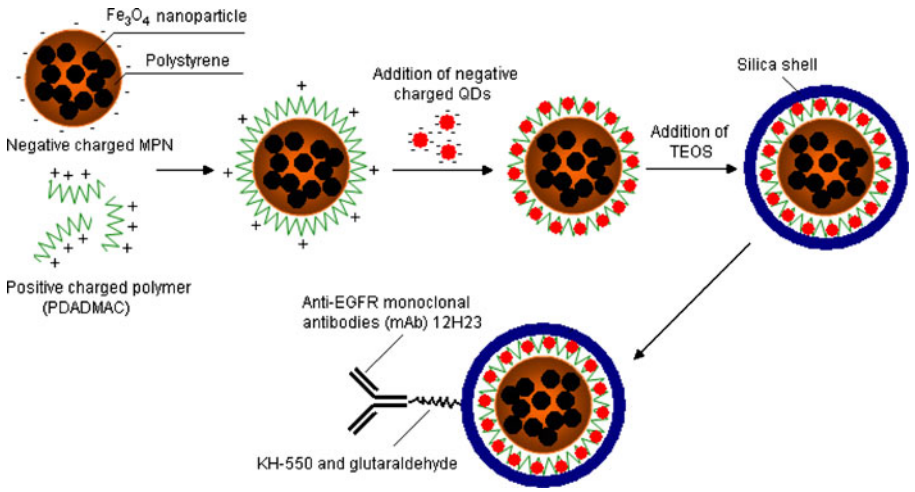

Fig. 1 Schematic illustration for the formation of silica-coated magneto-fluorescent nanoscale bioprobe

washed using the same method as described above. The washed precipitates were re-dispersed in water (100 μl), and incubated with TEOS (4 μl, 20% ethanol) at room temperature overnight. The MPN–QDs–SiO_2 nanocomposites were thus obtained.

Preparation of Bioconjugates

KH-550 dissolved in phosphate buffered saline (PBS; 10 μl, 3 pmol) was mixed with the MPN–QDs–SiO_2 suspension. After 2 h, the glutaraldehyde dissolved in PBS (10 μl, 3 pmol) was added to the mixture. A further 2 h later, PBS-dissolved anti-EGFR mAb 12H23 (10 μl, 3–5 pmol) was incubated with the mixture at 15 °C overnight. The mixture solution was centrifuged and the precipitate was dispersed in the L-15 and RPMI-1640 culture media without FCS, respectively.

Cell Experiments

MDA-MB-435S and SMMC-7721 cells were respectively cultured in L-15 and RPMI-1640 culture medium with 10% FCS and 1% antibiotic–antimycotic at 37 °C, in a chamber containing 5% CO_2. Before incubation with the nanocomposites, the culture media were removed and the cells were washed three times with PBS. The culture media-dispersed bioconjugates (approximately 1.25 pmol/l, reference to MPN–QDs–SiO_2 nanospheres) were added to the washed cells and incubated with the cells at 37 °C. One hour later, the cells were washed several times with PBS and imaged with an upright fluorescent microscope (Leica DME, Germany). As a control, the MPN–QDs–SiO_2 nanospheres without antibodies were incubated with the MDA-MB-435S and SMMC-7721 cells, and then washed and imaged under the same conditions as described above. To investigate the fluorescence stability of the QD bioconjugates on the cells, the MDA-MB-435S cells labeled with the MPN–QDs–SiO_2 antibodies were continuously excited by the upright fluorescent microscope with the light wavelength of 488 nm for 60 min. During the irradiation process, the fluorescent images of the cells were recorded. To compare specific and nonspecific binding, the nanocomposites with and without antibodies were incubated with the MDA-MB-435S cells ($n=3$) for 1 h. After washing and digestion, the cell precipitates were incubated with aqua regia (300 μl) for a week until the QDs in the MPN–QDs–SiO_2 nanospheres were completely dissolved into Cd and Te. The cell and aqua regia mixture solutions were then diluted to 3 ml with water, and the concentrations of Cd atoms in these solutions were measured using ICP-AES (IRIS-Advantage 1000; Thermo Jarrell Ash Co., USA). The cells that were not incubated with the nanocomposites were also mixed with aqua regia and further diluted with water for the ICP-AES measurement. In order to investigate whether the bioconjugates could separate the cancer cells, the MDA-MB-435S cells were digested with ethylenediaminetetraacetic acid (EDTA), precipitated by centrifugation and washed with PBS. The culture media-dispersed bioconjugates (approximately 1.25 pmol/l, with reference to MPN–QDs–SiO_2 nanospheres) were then added to the precipitates (cells), and incubated at 37 °C. One hour later, the cells were collected by magnetic separation, washed and imaged. As a control, the bioconjugates were incubated with the suspension-cultured K562 cells, which did not express EGFR and were collected by magnetic separation using the method described above.

Characterization of the Nanocomposites

The morphologies of the MPN, MPN–QDs and MPN–QDs–SiO_2 nanospheres were observed by transmission electron microscopy (TEM; JSM-6360LV, JEOL, Japan) and

scanning electron microscopy (SEM) equipped with energy-dispersive X-ray spectrometry (EDS; JEM-1200EX/S). The room temperature fluorescence spectra were measured on a fluorescence spectrometer (F-2500; Hitachi, Japan) with a xenon lamp source. To investigate the fluorescence stability of the MPN–QDs–SiO_2 nanospheres during storage, the nanosphere sample was placed at 4 °C in a refrigeratory, and its fluorescence was measured after 0, 3 and 7 days of storage. The zeta potential of the samples were measured using photon correlation spectroscopy (PCS; 3000HS, Malvern), and each sample was repeatedly measured five times.

Results and Discussion

TEM images of the MPN before and after coating with QDs and the silica shell are shown in Fig. 2. Each MPN has a pale shell and dark core. The magnified image clearly showed that a large amount of dark dots was embedded inside the MPN (see Fig. 2a, insert); these dark dots must be Fe_3O_4 nanoparticles (the properties of the same sample have been reported in our previous work [10]). After being coated with one layer of PDADMAC/QDs, the surfaces of MNP–QDs obtained were rougher than those of the uncoated MPN, and an obvious shell on each sphere could be observed clearly, indicating the success of the QD coating. Although the MPN and MPN–QDs had pale shells (PS and QDs) and dark cores (Fe_3O_4), the MPN–QDs, after being incubated with TEOS, exhibited more obvious core–shell structures. It is known that SiO_2 usually exhibits pale morphology through TEM observation compared with dark inorganic nanoparticles, and the enhanced pale shells on the MPN–QDs surface implied that the nanocomposites had been successfully coated with the silica shell. SEM images also show that the surfaces of MPN–QDs (Fig. 3b) and MPN–QDs–SiO_2 (Fig. 3c) were more rough than those of the MPN (Fig. 3a). The surfaces of MPN–QDs–SiO_2 were roughest among the three samples. The silica shell growing on the surface of MPN–QDs is a heterogeneous nucleation process. As substrates of nucleation for shell formation, however, the MPN–QDs are very large, and the microstructure details of MPN–QD surface are not uniform (Fig. 3b′). The growth rates of the silica shells on the different MPN–QD surface sites are therefore not symmetrical. This may be the main reason why some larger MPN–QDs–SiO_2 exhibited very rough surfaces. Coating with PDADMAC, QDs and the silica shell did not result in the obvious aggregation of nanoparticles. The magnified images of MPN–QDs (Fig. 3b′) and MPN–QDs–SiO_2 (Fig. 3c′) revealed that nearly the entire surface of the MPN (Fig. 3a′) was coated with shells. The size distribution of the MPN slightly shifted to a larger size after the MPN (Fig. 3a″) was coated with QDs and SiO_2 (Fig. 3b″ and c″), and the average diameters of the MPN, MPN–QDs and MPN–QDs–SiO_2 were about 746.12±583.34, 791.81±510.20 and 813.61±602.00 nm, respectively. EDS results (Fig. 4) indicated that MPN/QDs have C, Fe, O, Cd and Te, and MPN/QDs/SiO_2 have C, Fe, O, Cd, Te and Si chemical signals, which was different from those of the MPN where Cd, Te and Si signals were absent. The combined TEM, SEM and EDS data provided enough evidence of successful coating of QDs and silica shells onto the surfaces of the MPN.

The fluorescent properties are shown in Fig. 5. After being deposited on the surface of the MPN, the emission peak of QDs shifted from 650 to 688 nm. After being further coated with a silica shell, this emission peak shifted from 688 to 669 nm, and the emission intensity decreased at least 14.7%, when compared to the QDs (Fig. 5A(a)). The optical properties of the QDs were mainly dependent on surface state and size. The shifted emission wavelength and decreased emission intensity of the QDs may be caused by a

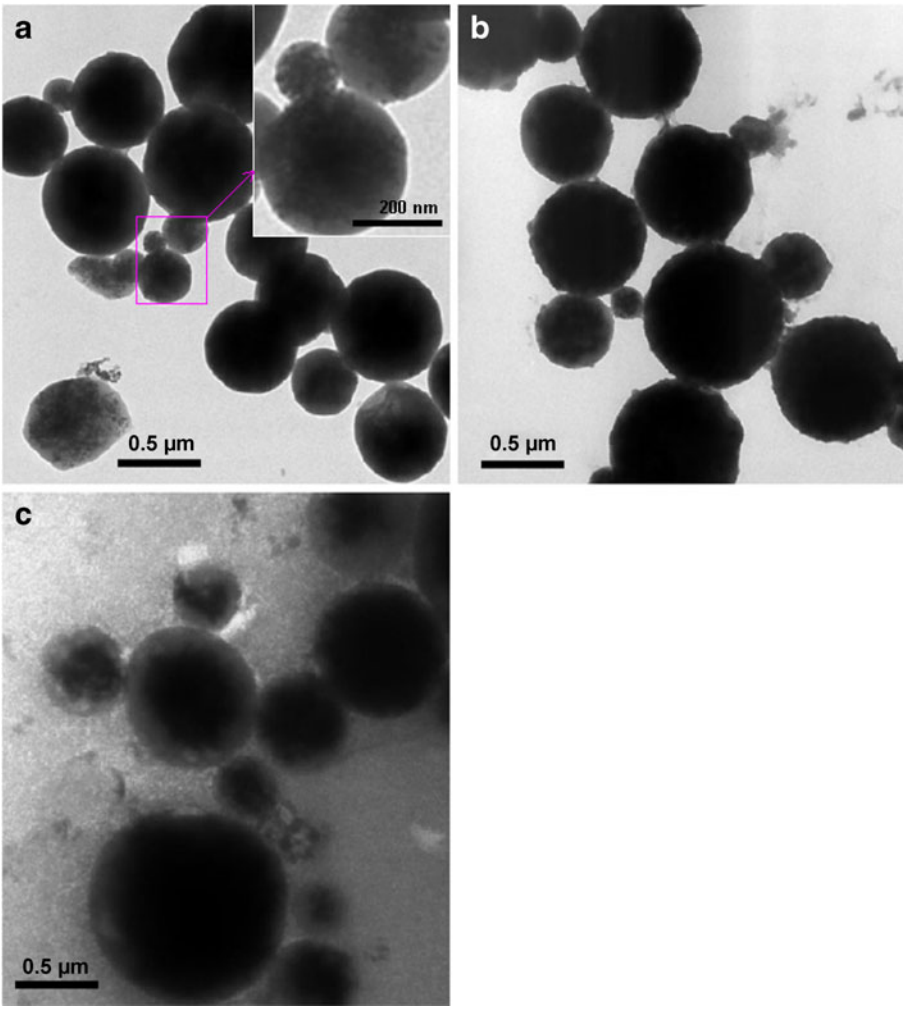

Fig. 2 TEM images of **a** magnetic polystyrene nanospheres (MPN), **b** MPN–quantum dots (MPN–QDs) and **c** MPN–QDs–SiO_2

change in the environment from water to a polymer (PDADMAC) and silica shell, and by the increased surface defects of QDs. Similar results have been reported by other researchers [20]. Although the optical properties of the QDs changed somewhat after being embedded into the polymer and silica shell, the MPN–QDs and MPN–QDs–SiO_2 obtained still emitted a bright fluorescence, which had a similar red color to the QDs observed. An interesting finding is that the fluorescent intensity of the MPN–QDs–SiO_2 slightly increased during a week of storage (Fig. 5B). It is known that the crystalline structure of just synthesized SiO_2 will be Ostwald ripened after storage for several days. The slightly increased fluorescent intensity may be due to some nonradiative recombination sites on the surface of the QDs were passivated by the aging silica shell. This indicates that the fluorescence of the MPN–QDs–SiO_2 was stable during at least a week of storage.

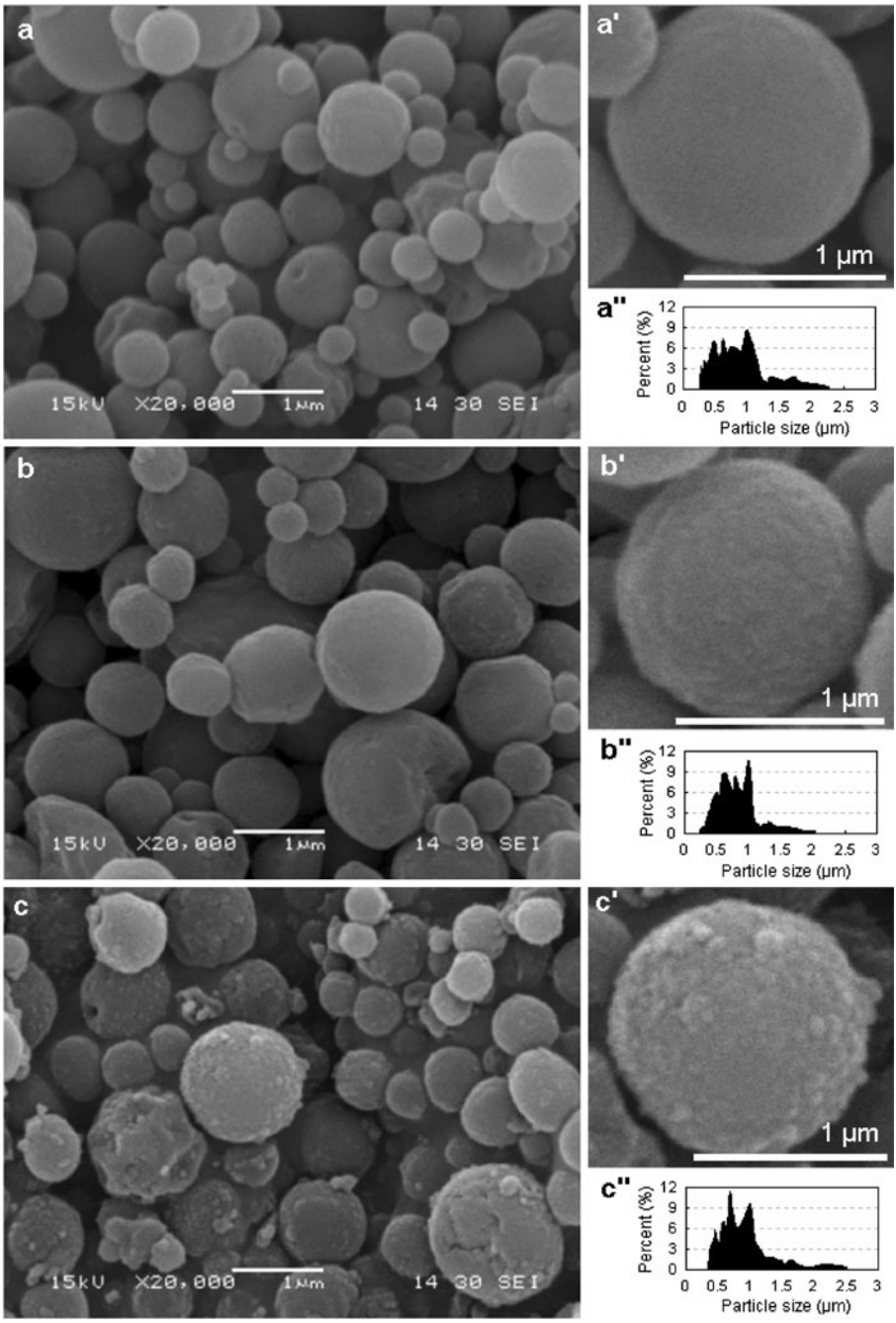

Fig. 3 SEM images and size distributions of **a**, **a′**, **a″** MPN; **b**, **b′**, **b″** MPN–QDs; and **c**, **c′**, **c″** MPN–QDs–SiO_2. For a clear observation of the surfaces of the nanoparticles, a larger particle was selected (**a′**, **b′** and **c′**) from each corresponding original image (**a**, **b** and **c**) and its image was magnified

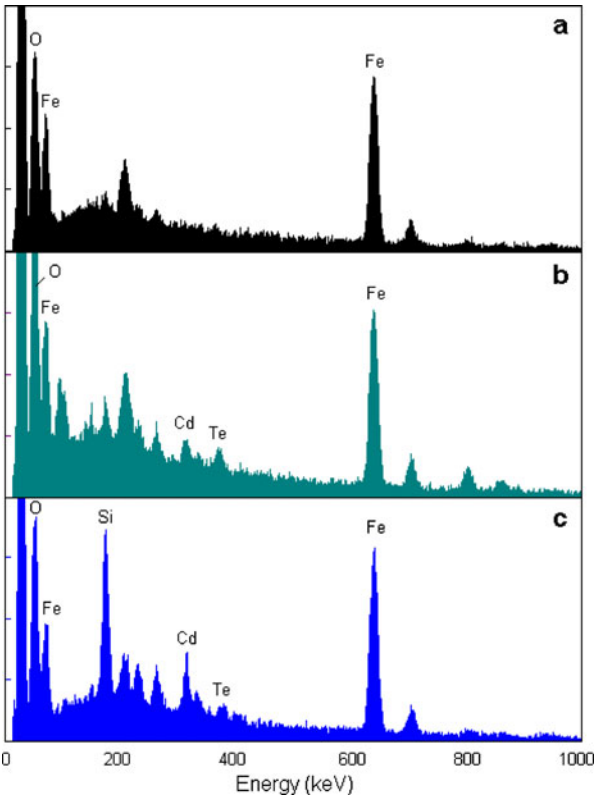

Fig. 4 EDS spectra of **a** MPN, **b** MPN–QDs and **c** MPN–QDs–SiO_2

The zeta potential of the MPN–QDs was −18.67±6.95 meV. After being coated with a silica shell, the zeta potential slightly improved to −24.22±5.41 meV. The negatively charged silica shell may cause the improved negative zeta potential. It is known that the cells usually have a negatively charged surface. The improved negative zeta potential of the MPN–QDs–SiO_2 may be beneficial for improving the electrostatic repulsion between nanocomposites and cells. Additionally, the silica shell also provided a spatial obstacle, so that the nonspecific binding between the nanocomposites and cells was reduced.

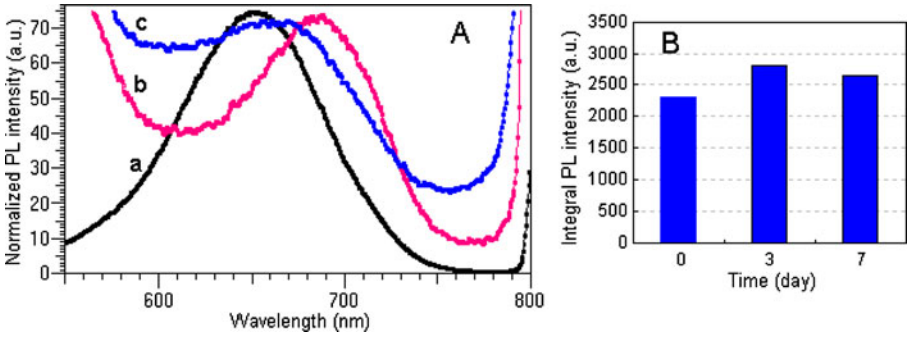

Fig. 5 **A** Photoluminescent (PL) spectra of **a** QDs, **b** MPN –QDs and **c** MPN–QDs–SiO_2. **B** Integral PL intensity (the wavelength between 600 and 750 nm) of the MPN–QDs–SiO_2 varying with storage time at 4 °C

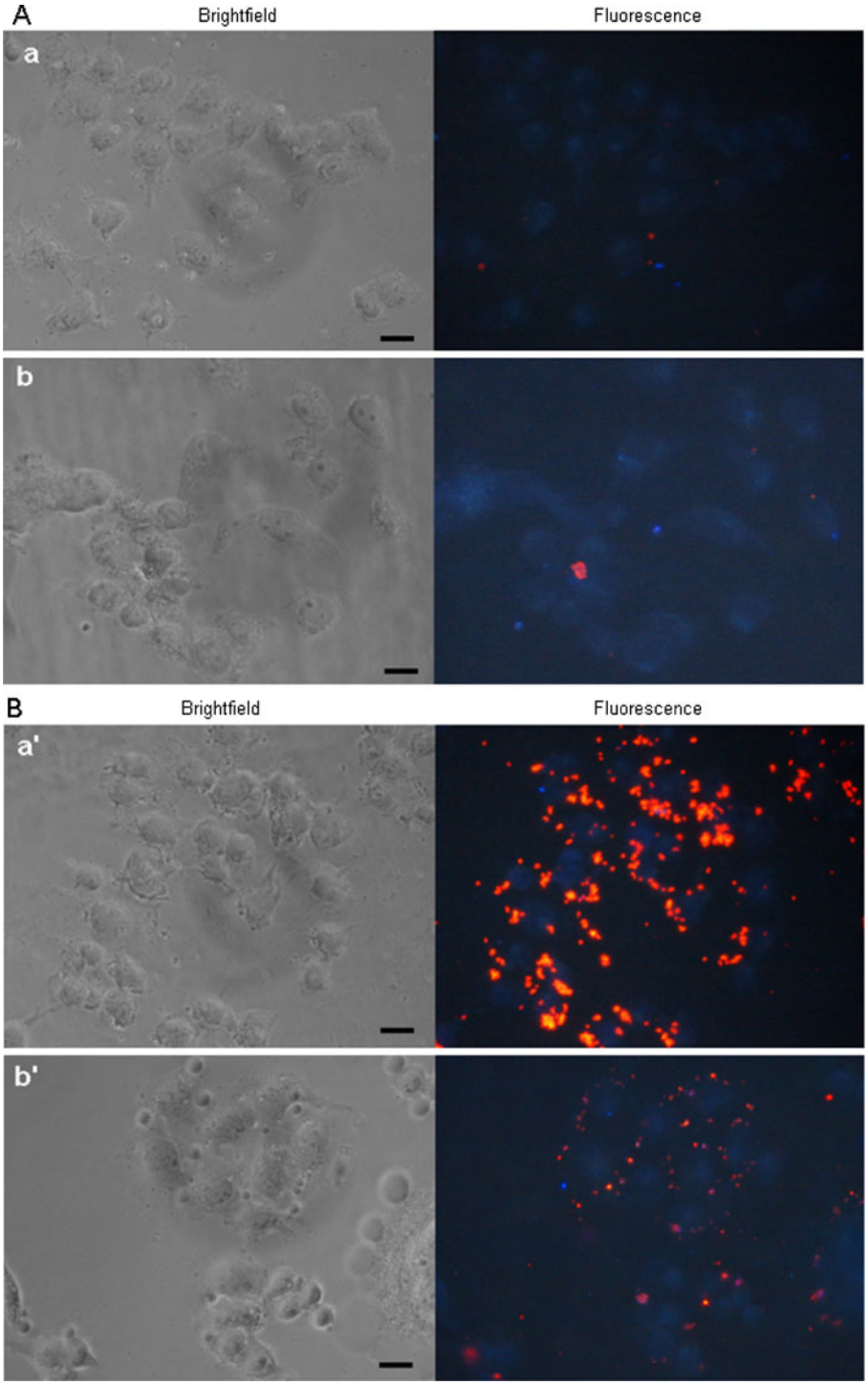

Fig. 6 Cancer cells incubated with **A** MPN–QDs–SiO_2 and **B** MPN–QDs–SiO_2 antibodies. **a, a′** MDA-MB-435S cancer cells; **b, b′** SMMC-7721 cells. Bar, 10 μm

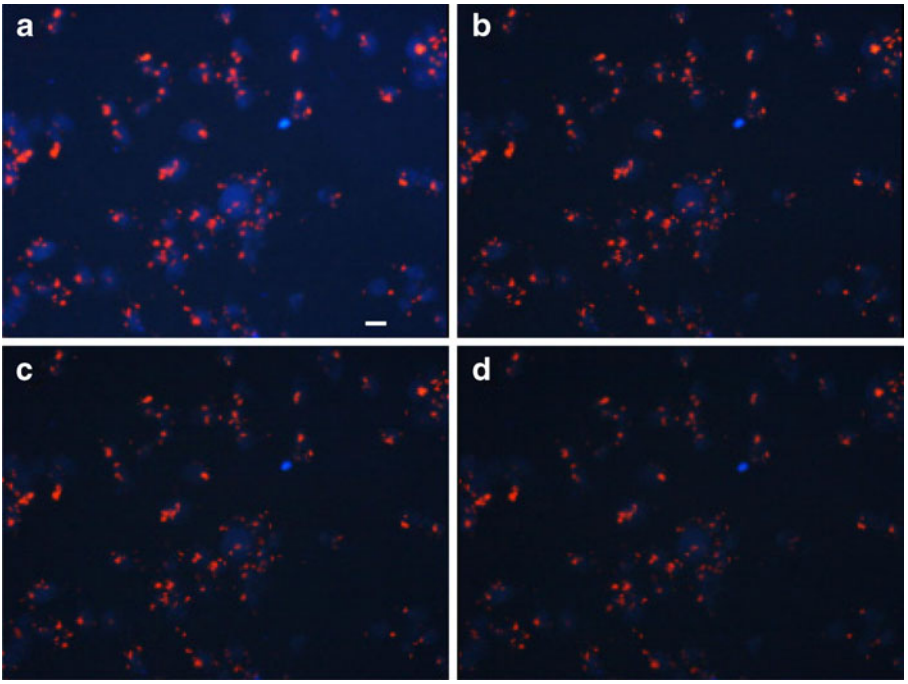

Fig. 7 Fluorescence stability of MPN–QDs–SiO_2 antibodies on the surface of MDA-MB-435S cancer cells. The cells were continuously excited by the upright fluorescent microscope with the light wavelength of 488 nm. The cells were excited for **a** about 30 s, **b** 15 min, **c** 30 min and **d** 60 min, respectively. Bar, 10 μm

When the cancer cells (MDA-MB-435S and SMMC-7721) were incubated with the MPN–QDs–SiO_2 nanocomposites for 1 h and subsequently washed with PBS, very little red fluorescence could be observed on the cells (Fig. 6A(a, b)). When the nanoparticles were conjugated with antibodies, however, a large amount of red fluorescent spots could be observed in the field of view after the cancer cells were incubated with the bioconjugates. Each cell was labeled with the fluorescent nanoparticles (Fig. 6B(a′, b′)). The fluorescence of the MPN–QDs–SiO_2 antibodies on the surface of cancer cells was fairly stable. As shown in Fig. 7, when the MDA-MB-435S cells labeled with the MPN-QDs-SiO_2-

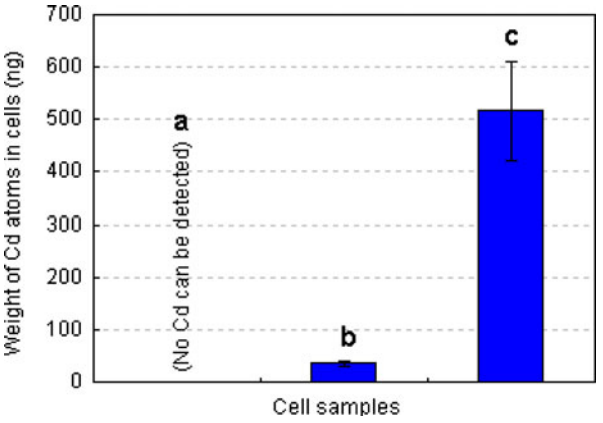

Fig. 8 The amount of Cd atoms in MDA-MB-435S cells. **a** Pure cells, **b** cells incubated with MPN–QDs–SiO_2 and **c** cells incubated with MPN–QDs–SiO_2 antibodies

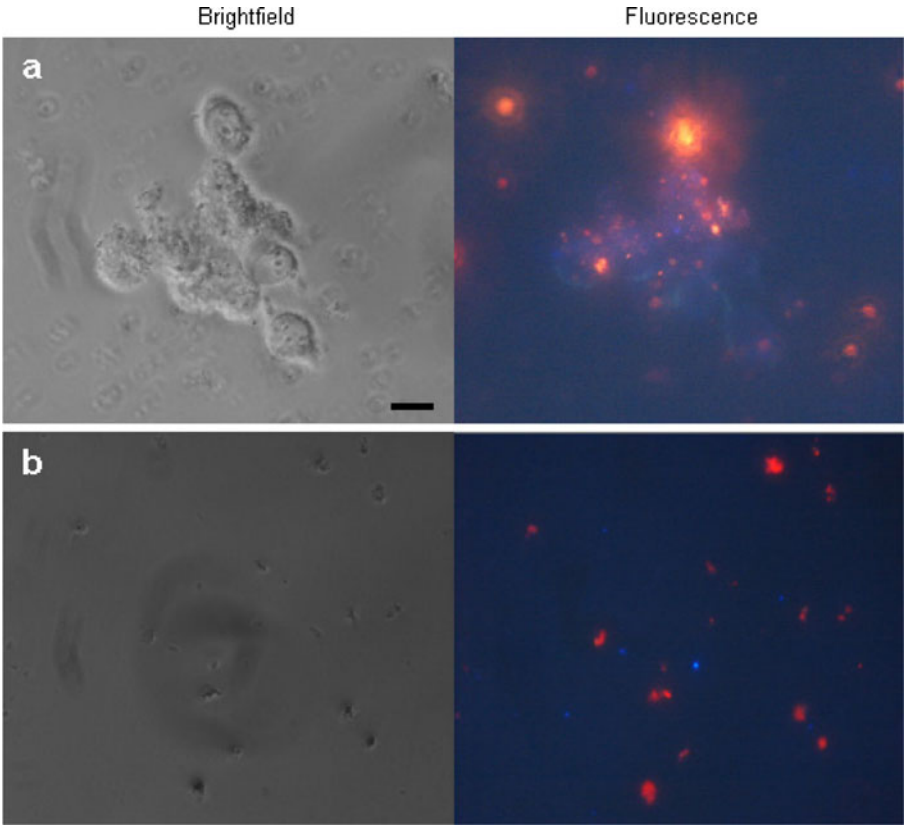

Fig. 9 **a** Suspended MDA-MB-435S cancer cells digested with EDTA, labeled and collected with MPN–QDs–SiO_2 antibodies. **b** Suspended K562 cells could not be collected by the MPN–QDs–SiO_2 antibodies and K562 cells could not be observed around the fluorescent nanocomposites. Bar, 10 μm

antibodies were continuously excited by the fluorescent microscope light with the wavelength of 488 nm for 15, 30 and 60 min, respectively, the nanoparticle fluorescence on the cells did not obviously change compared with that on the cells excited for about 30 s. This is beneficial for long-term observation. Since each nanocomposite had a large amount of Cd-containing QDs, the quantity of Cd atoms in cells can be used for judging the relative amount of nanocomposites specifically and nonspecifically captured by cells. As shown in Fig. 8, the Cd atoms in cells that were not incubated with nanocomposites could not be detected by the ICP-AES. Compared to the cells incubated with the nanocomposites in the absence of antibodies, the cells incubated with the bioconjugates had more Cd atoms, at least 14.63-fold greater. This result further indicated that the labeling of the cancer cells by bioconjugates was based on the antibody–antigen interaction, with nonspecific binding inappreciable. Since the nanocomposites contained magnetic nanoparticles, the bioconjugates can also be used for specifically separating target cells. In order to demonstrate this, the MDA-MB-435S cells were digested with EDTA and the suspended cells obtained were incubated with the bioconjugates in the L-15 culture medium without FCS. It is known that the activity of antigens on the cell surface are usually not obviously reduced after being treated with EDTA alone; therefore, nearly each the suspended cancer cells were labeled with the bioconjugates,

and the labeled cells could be collected quickly by absorption with a small magnet (Fig. 9a). As a control, however, when the bioconjugates were incubated with the suspended K562 cells and subsequently absorbed with the magnet using the same method described above, no cells could be observed beside the collected nanocomposites (Fig. 9b).

In summary, the surfaces of magnetically modified polystyrene nanospheres (Fe_3O_4 nanoparticles incorporated into the spheres) were electrostatically deposited with QDs and subsequently coated with a silica shell. Compared with the uncoated spheres, the silica-coated spheres had improved negative zeta potential and a spatial obstacle, which may be the main reason why nonspecific binding between the silica-coated spheres and cancer cells was significantly reduced. After the silica-coated spheres were conjugated with anti-EGFR, the bioconjugates could recognize liver cancer cells (SMMC-7721) and breast cancer cells (MDA-MB-435S), as EGFR was highly expressed on the surface. The bioconjugates could also quickly separate these cancer cells via magnetic force. If the cells did not express EGFR, as was the case with K562 cells, these bioconjugates could not recognize and separate them. The novel nanocomposites conjugated with antibodies prepared in this work may be of interest for use in cancer diagnosis in the future.

Acknowledgement This work was supported in part by the National High Technology R&D Program of China (863 Program, No. 2007AA03Z319), the Key Technologies R&D Program in the 11th Five-year Plan of China (2009ZX09103-701), the National Natural Science Foundation of China (No. 30870711) and the Nanoscience Foundation of Shanghai (0952nm04700).

References

1. Bruchez, M., Moronne, M., Gin, P., Weiss, S., & Alivisatos, A. P. (1998). Semiconductor nanocrystals as fluorescent biological labels. *Science, 281*(5385), 2013–2016.
2. Chan, W. C. W., & Nie, S. M. (1998). Quantum dot bioconjugates for ultrasensitive nonisotopic detection. *Science, 281*(5385), 2016–2018.
3. Michalet, X., Pinaud, F. F., Bentolila, L. A., Tsay, J. M., Doose, S., Li, J. J., et al. (2005). Quantum dots for live cells, in vivo imaging, and diagnostics. *Science, 307*(5709), 538–544.
4. Chomoucka, J., Drbohlavova, J., Huska, D., Adam, V., Kizek, R., & Hubalek, J. (2010). Magnetic nanoparticles and targeted drug delivering. *Pharmacological Research, 62*(2), 1–6.
5. van Landeghem, F. K., Maier-Hauff, K., Jordan, A., Hoffmann, K. T., Gneveckow, U., Scholz, R., et al. (2009). Post-mortem studies in glioblastoma patients treated with thermotherapy using magnetic nanoparticles. *Biomaterials, 30*(1), 52–57.
6. Bruns, O. T., Ittrich, H., Peldschus, K., Kaul, M. G., Tromsdorf, U. I., Lauterwasser, J., et al. (2009). Real-time magnetic resonance imaging and quantification of lipoprotein metabolism in vivo using nanocrystals. *Nature Nanotechnology, 4*(3), 193–201.
7. Yan, H., Zhang, J. C., Yu, B. W., & Shen, Y. (2010). Preparation and formation mechanism of nanocomposites with fluorescent and magnetic properties. *Acta Materialia, 58*, 58726–58733.
8. Shi, D., Cho, H. S., Chen, Y., Xu, H., Gu, H., Lian, J., et al. (2009). Fluorescent polystyrene-Fe_3O_4 composite nanospheres for in vivo imaging and hyperthermia. *Advanced Materials, 21*, 211–214.
9. Gao, J., Zhang, W., Huang, P., Zhang, B., Zhang, X., & Xu, B. (2008). Intracellular spatial control of fluorescent magnetic nanoparticles. *Journal of the American Chemical Society, 130*(12), 3710–3711.
10. Chu, M., Song, X., Cheng, D., Liu, S., & Zhu, J. (2006). Preparation of the quantum dots-coated magnetic polystyrene nanospheres for cancer cells labeling and separation. *Nanotechnology, 17*, 3267–3273.
11. Mendelsohn, J. (2002). Targeting the epidermal growth factor receptor for cancer therapy. *Journal of Clinical Oncology, 20*(18 Suppl), 1S–13S.
12. Arteaga, C. L. (2002). Overview of epidermal growth factor receptor biology and its role as a therapeutic target in human neoplasia. *Seminars in Oncology, 29*(5 Suppl 14), 3–9.

13. Nicholson, R. I., Gee, J. M., & Harper, M. E. (2001). EGFR and cancer prognosis. *European Journal of Cancer, 37*(Suppl 4), S9–S15.
14. Carteni, G., Fiorentino, R., Vecchione, L., Chiurazzi, B., & Battista, C. (2007). Panitumumab a novel drug in cancer treatment. *Annals of Oncology, 18*(Suppl 6), 16–21.
15. Zhang, W., Gordon, M., & Lenz, H. J. (2006). Novel approaches to treatment of advanced colorectal cancer with anti-EGFR monoclonal antibodies. *Annals of Medicine, 38*(8), 545–551.
16. Luwor, R. B., Johns, T. G., Murone, C., Huang, H. J., Cavenee, W. K., Ritter, G., et al. (2001). Monoclonal antibody 806 inhibits the growth of tumor xenografts expressing either the de2-7 or amplified epidermal growth factor receptor (EGFR) but not wild-type EGFR. *Cancer Research, 61*(14), 5355–5361.
17. Scott, A. M., Lee, F. T., Tebbutt, N., Herbertson, R., Gill, S. S., Liu, Z., et al. (2007). A phase I clinical trial with monoclonal antibody ch806 targeting transitional state and mutant epidermal growth factor receptors. *Proceedings of the National Academy of Sciences of the United States of America, 104*(10), 4071–4076.
18. Johns, T. G., Adams, T. E., Cochran, J. R., Hall, N. E., Hoyne, P. A., Olsen, M. J., et al. (2004). Identification of the epitope for the epidermal growth factor receptor-specific monoclonal antibody 806 reveals that it preferentially recognizes an untethered form of the receptor. *The Journal of Biological Chemistry, 279*(29), 30375–30384.
19. Chu, M., Wu, Q., Yang, H., Yuan, R., Hou, S., Yang, Y., et al. (2010). Transfer of quantum dots from pregnant mice to pups across the placental barrier. *Small, 6*(5), 670–678.
20. Wang, D., Rogach, A. L., & Caruso, F. (2002). Semiconductor quantum dot-labelled microsphere bioconjugates prepared by stepwise self-assembly. *Nano Letters, 2*(8), 2857–2861.